

## Hotspot Angle Grids for Radiation Transfer

For plasmas in which non-local radiation-dependent rates are important for level populations, each plasma cell must sample its surroundings using an angle grid of rays emanating from its centroid. *SPECT3D* implements the method of discrete ordinates [1] for determining angle grids for radiation transfer. With this method, each cell uses an angle grid which treats all directions equally. However, this is not well suited to a problem where the important radiation comes from a certain hotspot region of the plasma. To study this, we use a plasma grid in 2DRZ geometry where a hot D2Ar core emits radiation, which in turn photopumps  $K\alpha/\beta$  emission in a CHCu shell further out. Contour slice plots of material density for a 40×40-node example are shown in Figure 1a for the D2Ar core, and Figure 1b for the CHCu shell.

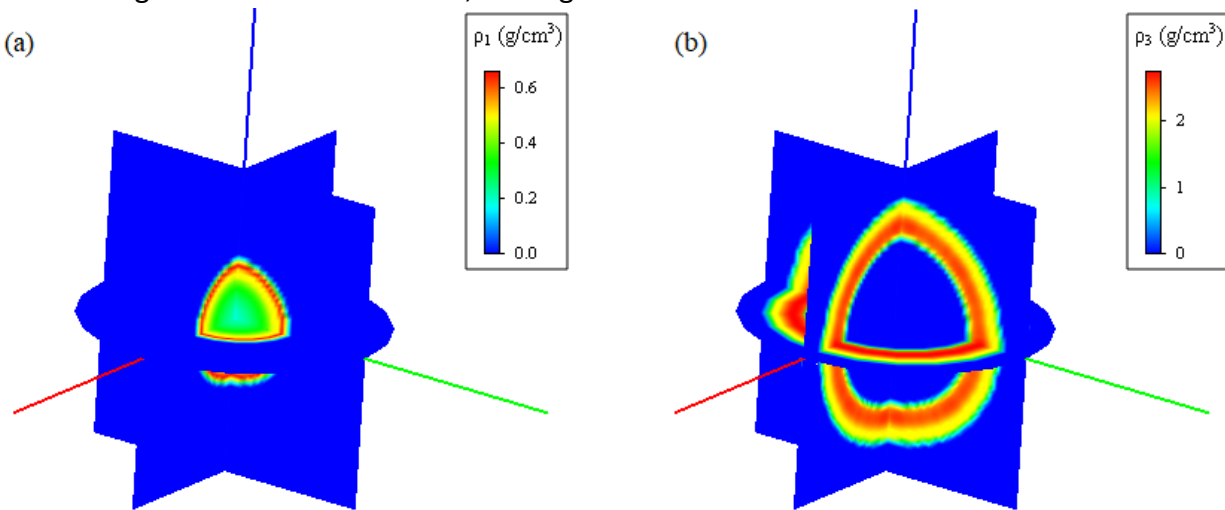


Figure 1. Spatial contour slice density plots of (a) hot D2Ar core, and (b) CHCu shell. R extends to 0.02 cm, and Z extends from -0.02 to 0.02 cm.

When the standard method of discrete ordinates is used in this case, large variation is seen in the photopumped  $K\alpha$  (8047 eV) emission from the Cu in the CHCu shell. Figure 2 shows images of the  $K\alpha$  emission, calculated by *SPECT3D* using the short characteristics (SC) method of radiation transfer, with the four levels of the discrete ordinates method for angle grids, where SN2 uses the smallest number of angles, and SN8 uses the most. The  $K\alpha$  emission comes from the spherical CHCu region, and the central hotspot is also visible at this energy. In all cases, the  $K\alpha$  emission from the Cu in the shell is not distributed uniformly, owing to the discretization of the angle grid. Indeed, the shape of the distribution depends on the particular angle grid used. This is because, in certain regions, the angle grid reaches the radiation hotspot for some angles, while other regions do not. Similar behavior is seen when using long characteristics (LC).

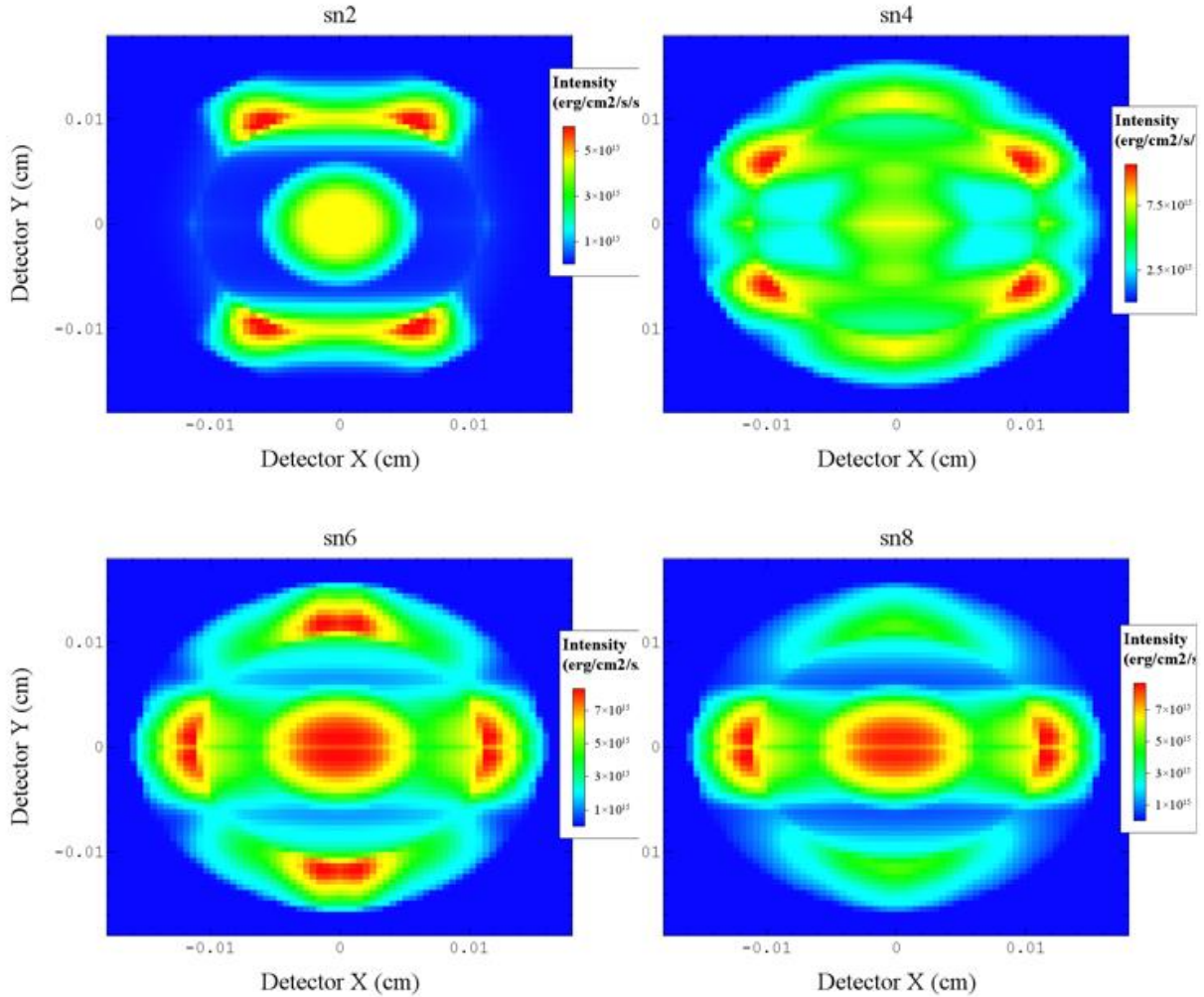


Figure 2. Images of 8047 eV photon energy ( $K\alpha$  emission), calculated by SPECT3D, from the CHCu shell in a  $40 \times 40$  spatial grid using the SC model ( $N=3$ ) with four SN angle grids.

In order to resolve the hotspot in all regions of the plasma, a new angle grid model was implemented which focuses radiative transfer rays onto a defined spherical hotspot centered on the origin. When using this model, the user firstly provides the number of angles for the “hotspot grid”, which resolves the solid angle subtended by the hotspot, looking both *toward* and *away from* the hotspot. This was done to fit into the existing code framework, which defines rays in only the positive-y space, and then uses both positive and negative directions for rays. Secondly, the user provides the number of angles for the “remainder grid”, which resolves the remaining solid angle. Thus, the user inputs the following:

$r_{HS}$ : Radius of the hotspot (cm) vs. time.

$\phi$ : Number of grid angles *around* the vector pointing to the origin, used by both the hotspot and remainder grids.

$\theta_{HS}$ : Number of hotspot grid angles stepping *away from* the vector pointing to the origin. This grid gets drawn toward and away from the hotspot, and thus gets drawn twice.

$\theta_{rem}$ : Number of remainder grid angles stepping *away from* the vector pointing to the origin.

Thus, each plasma cell gets a unique grid, each resolving the hotspot with the same number of rays. An example angle grid is shown in Figure 3. Each point represents the end of a unit vector eliminating from the cell centroid. The lines between points are to aid the eye. The red points resolve the solid angle pointing at the hotspot, and also directly away from the hotspot. While only positive directions are shown, negative directions are also computed, which completes the solid angle. This grid is meant for display purposes and has more angles than a user should need.

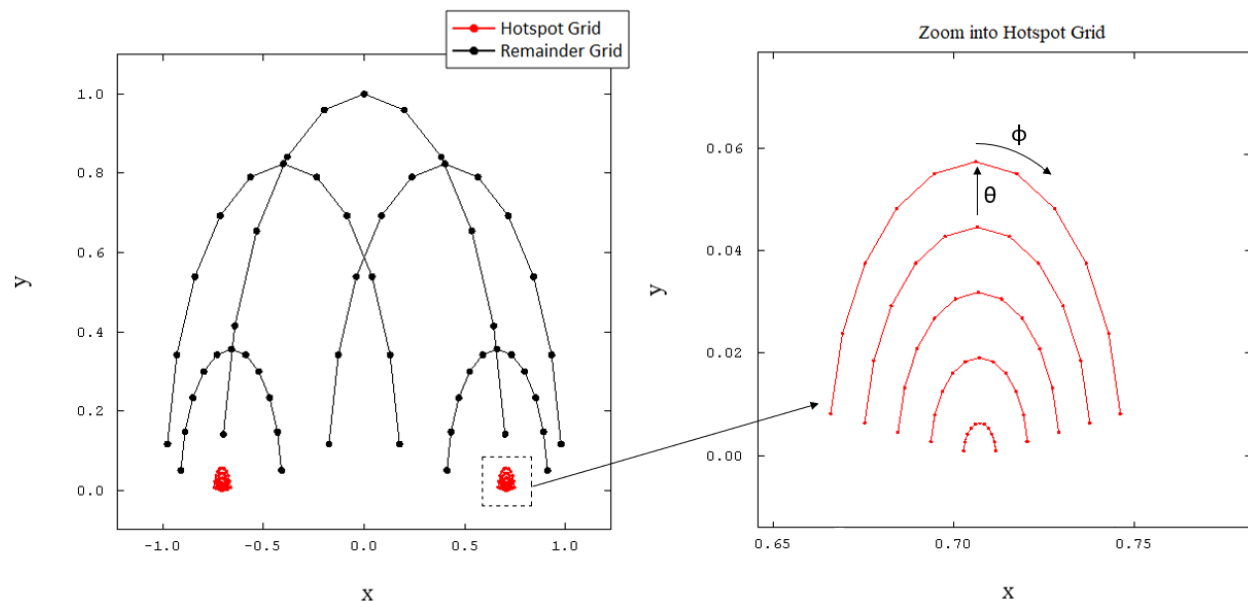


Figure 3. Example hotspot (red) and remainder (black) angle grid for a zone near the x-axis, plotted in the XY plane, with a zoom onto a hotspot portion shown on the right.

Each section of the angle grid begins at half of an angle step. Thus, there are no angles which point directly at the boundary between hotspot and remainder solid angle sections, nor is there a ray which points directly at the hotspot center. Since both positive and negative ray directions are used, and since the hotspot grid is drawn in both directions, the total number of angles used by each zone is defined by:

$$N_{\text{angles}} = 2\phi ( 2\theta_{HS} + \theta_{rem} )$$

For reference, the standard SN6 model uses a total of 48 angles. When using SC, it is recommended to use a similar number of total angles, since ray boundary conditions rely on finding the closest angle. E.g., when using the hotspot grid method, a value of 3 for all three angle grid inputs will also result in 48 total angles. The calculation time will typically be proportional to the number of angles.

Note that the grid shown in Figure 3 is an example for a cell whose centroid lies outside the hotspot radius. Cells whose centroid lies inside the hotspot receive a grid with the same total number of angles which are distributed evenly in  $\phi$  and  $\theta$ , without any division into “hotspot” and “remainder” grids (thus there is no subscript on  $\theta$ ).

## Results

When the hotspot angle grid model is used, radiation from the hot core is more consistently transferred to surrounding plasma cells. This is demonstrated for both LC and SC ( $N=3$ ) in Figures 4-7, which show images of the  $K\alpha$  emission, calculated by *SPECT3D* using the new hotspot grid model with  $r_{HS} = 0.0057$  cm, and  $\phi = \theta_{HS} = \theta_{rem} = 3$ . The number of spatial plasma grid nodes is  $10\times 10$ ,  $15\times 15$ ,  $40\times 40$ , and  $70\times 70$  for Figures 4, 5, 6, and 7, respectively. Each grid has a temperature, density, and material distribution similar to the one shown in Figure 1. In each of Figure 4-7, the LC calculation (a) is considered a benchmark for its corresponding SC calculation (b). Especially in the  $40\times 40$  and  $70\times 70$  grids, the  $K\alpha$  emission is observed very uniformly from the CHCu shell. The  $40\times 40$  case can be compared directly to the result from the SN models in Figure 2, demonstrating a significant improvement in the radiation transport calculation. It is also significant that the SC result is nearly indistinguishable from the benchmark LC result in the  $40\times 40$  and  $70\times 70$  grids. In the much coarser grids of  $15\times 15$  and  $10\times 10$ , granularity in results is seen, and SC begins to disagree more with LC. Note that in each of Figures 4-7, the color scale is the same between (a) and (b), though this scale is not the same between figures. The scale is chosen to highlight the  $K\alpha$ -emitting shell, while the hot core is saturating the color scale at this photon energy.

In order to achieve this level of accuracy for SC, additional corrections were required. These, along with recommendations for choosing input parameters, are described in the following sections.

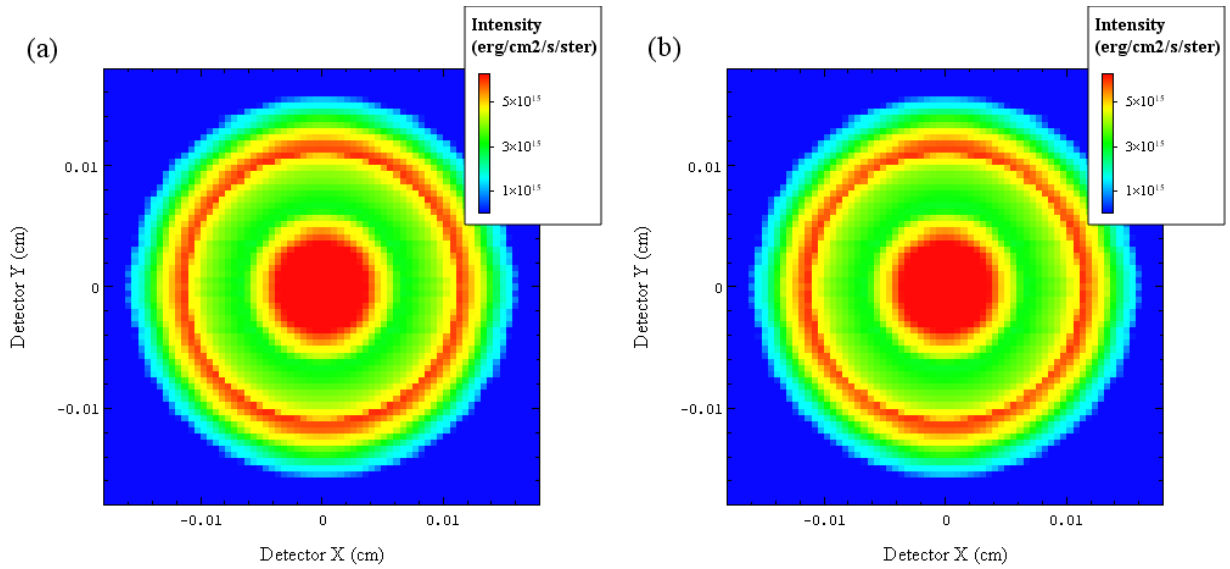


Figure 4.  $K\alpha$  emission images calculated by SPECT3D for  $70 \times 70$  spatial grid using hotspot angle grid model with  $r_{HS} = 0.0057$  cm, and  $\phi = \theta_{HS} = \theta_{rem} = 3$  for (a) LC, and (b) SC ( $N=3$ ).

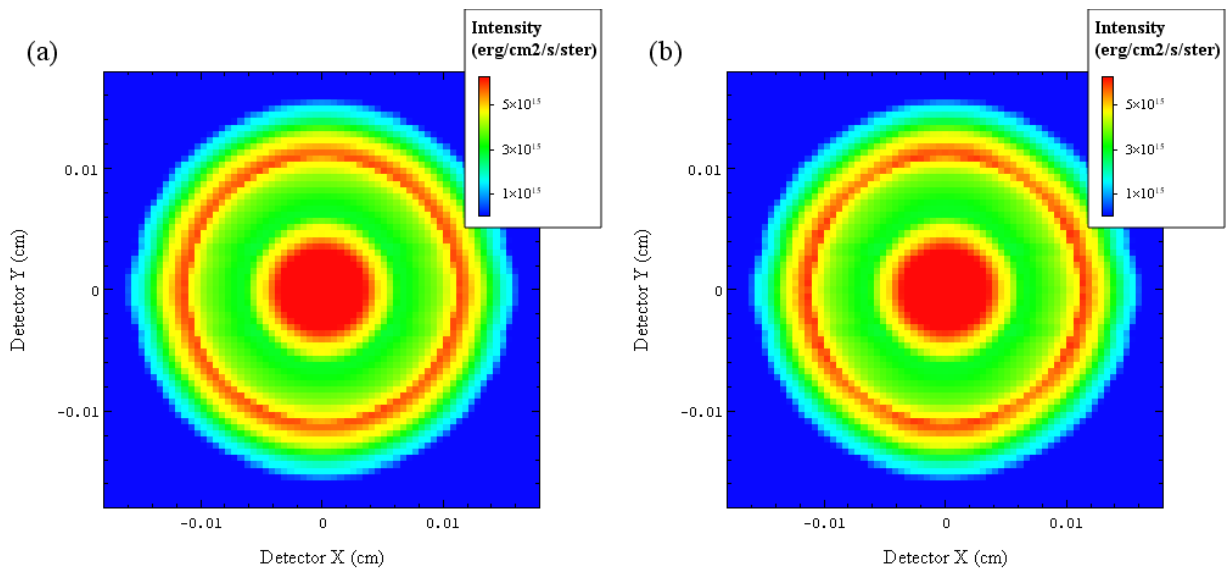


Figure 5.  $K\alpha$  emission images calculated by SPECT3D for  $40 \times 40$  spatial grid using hotspot angle grid model with  $r_{HS} = 0.0057$  cm, and  $\phi = \theta_{HS} = \theta_{rem} = 3$  for (a) LC, and (b) SC ( $N=3$ ).

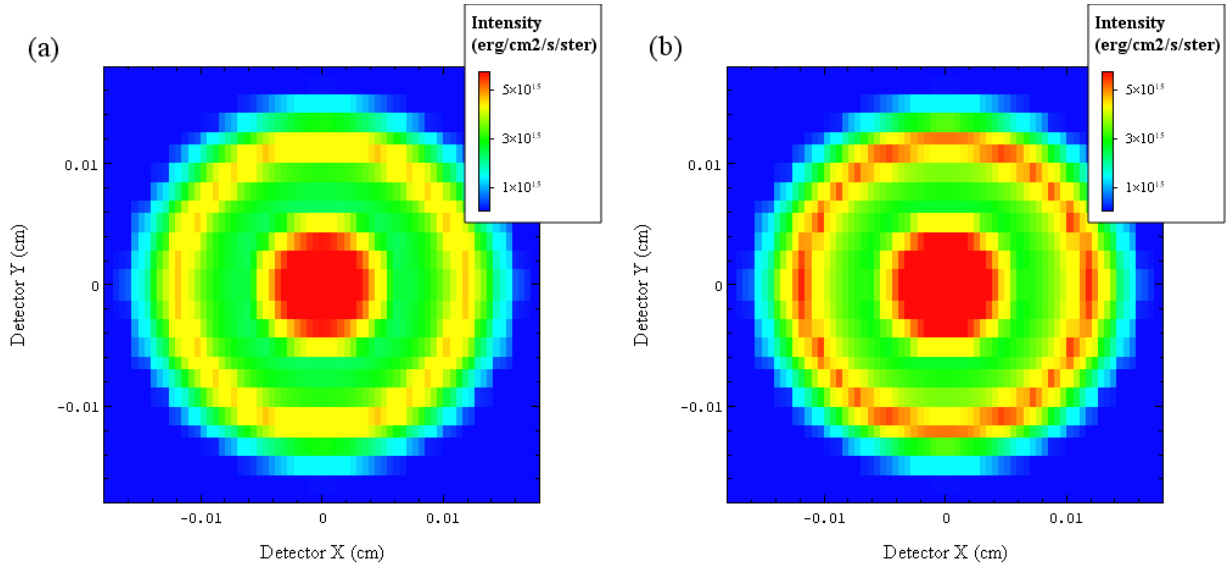


Figure 6.  $K\alpha$  emission images calculated by SPECT3D for  $15 \times 15$  spatial grid using hotspot angle grid model with  $r_{HS} = 0.0057$  cm, and  $\phi = \theta_{HS} = \theta_{rem} = 3$  for (a) LC, and (b) SC ( $N=3$ ).

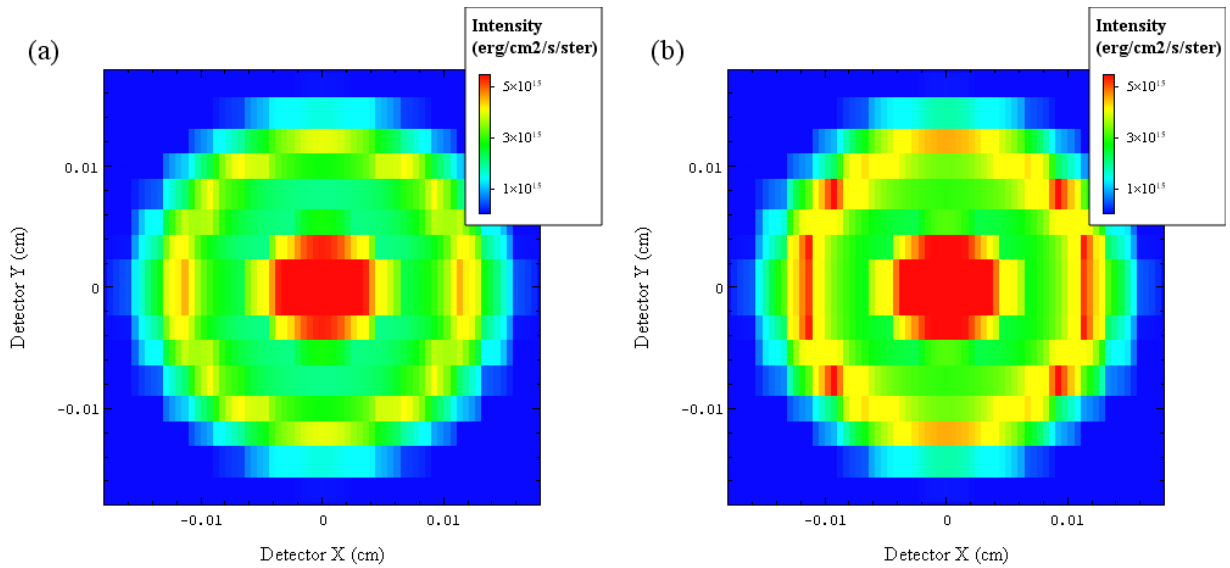


Figure 7.  $K\alpha$  emission images calculated by SPECT3D for  $10 \times 10$  spatial grid using hotspot angle grid model with  $r_{HS} = 0.0057$  cm, and  $\phi = \theta_{HS} = \theta_{rem} = 3$  for (a) LC, and (b) SC ( $N=3$ ).

### Path Length Correction for Short Characteristics Boundary Conditions

SC radiation transfer works from the edge of the plasma (where radiation is known) inward, explicitly calculating radiation transfer in steps of  $N$  cell intersections, where  $N$  is set by the user. Each plasma zone has its own grid of rays (angles). For each ray, beginning with its boundary condition at the  $N$ th cell intersection, radiation transfer is calculated through  $N$  cells, then to its start zone's centroid, and then further to the end of that zone, to be used as a

boundary condition for the beginning of another ray's N-step transfer. Consequently, the effective path to zone centroids inside the plasma is a jagged sequence of N-step segments, as opposed to the straight path from the plasma edge as in LC. We find that applying a multiplicative correction to the radiation boundary condition intensity, based on the ratio of the SC path to the LC path, does an excellent job at reproducing LC benchmarks. This is especially true when the important radiation experiences low optical depth. For high optical depth, boundary conditions are not important, so the scaling has no effect. For medium optical depths, accuracy is similar with and without the scaling technique. A benchmark study of these situations is provided in the Appendix "Boundary Condition Scaling for Short Characteristics in SPECT3D". In the current case of the hotspot angle grid model, this correction works best when this pathlength correction is based only on path length through the hotspot. This is illustrated in Figure 8. The gridlines are the plasma zone boundaries, for the 40×40-node example shown previously, in the RZ plane. The orange circle is the radius of the hotspot. The red line is a concatenation of the SC (N=3) ray segments which ultimately make their way from the plasma edge (out of view) to the "start zone" which is bordered in magenta. Each segment has 3 intersection points, after which its intensity value becomes the boundary value which begins the next segment. Upon reaching the start zone's centroid, it will have calculated the intensity for one of the rays in the angle grid for this start zone. The blue line is the straight path which that particular ray would take through the plasma in the LC method. Each of the red and blue lines is emboldened where it is inside the hotspot radius. Since this is a projection onto the RZ plane, the bold parts do not appear to line up with the radius. See that, in general, the total path through the hotspot is not the same between SC and LC. This is why a scaling of the SC boundary values can serve as a correction for SC.

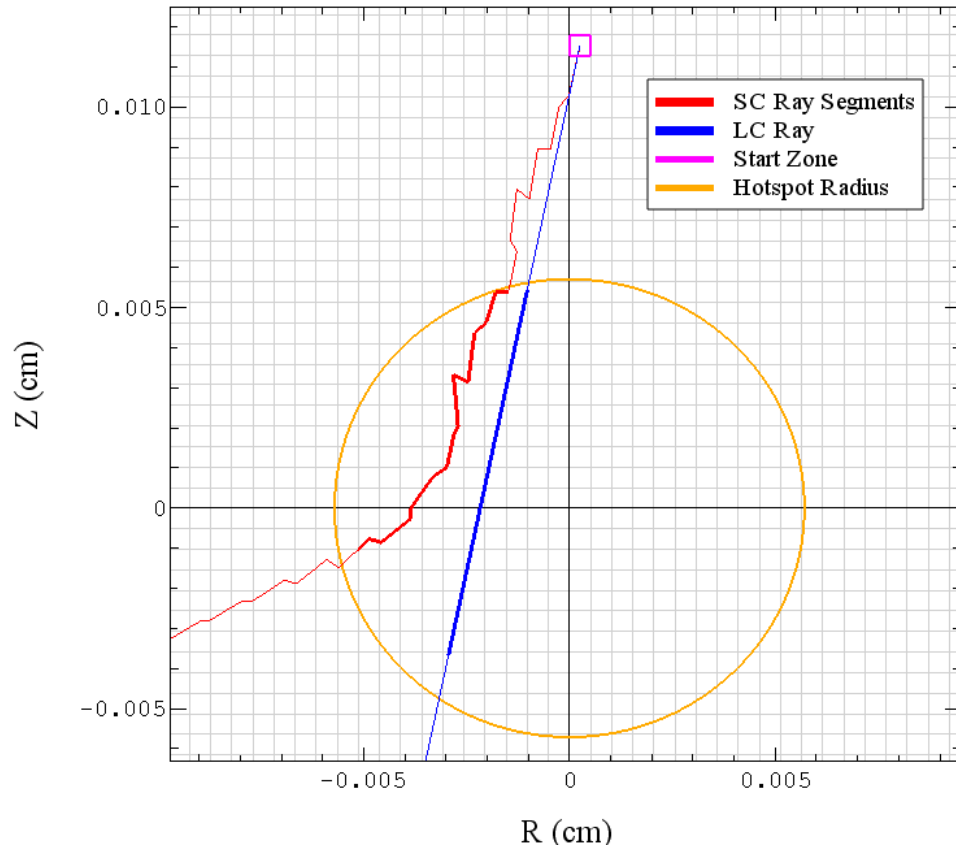


Figure 8. Example paths of SC (N=3) and LC paths in the 40x40 plasma. Paths are bold where they are inside the hotspot. Gridlines are plasma cell boundaries.

To accomplish this, each time a boundary value is used, it is scaled by this ratio:

$$\frac{\delta 1(\text{start zone})}{\delta 2(\text{boundary zone})}$$

where  $\delta 1$ , referring to the start zone, is the distance from the plasma edge to the end of the SC ray segment, *intersected with the hotspot sphere*, and  $\delta 2$ , referring to the boundary zone, is the distance from the plasma edge all the way through the cell, to the point where its intensity value becomes the start zone ray's boundary value, *intersected with the hotspot sphere*. Examples of these lengths are shown in Figure 9. Note that, though these path lengths to the plasma edge are stored, radiation transfer is not calculated all the way along them as it would be with LC. Since a given cell and ray intensity can only be calculated once a BC is known, each boundary value is always pre-corrected. I.e., the path length used in the calculation of each boundary value is scaled to the correct path length (from the plasma edge, intersected with the hotspot sphere).



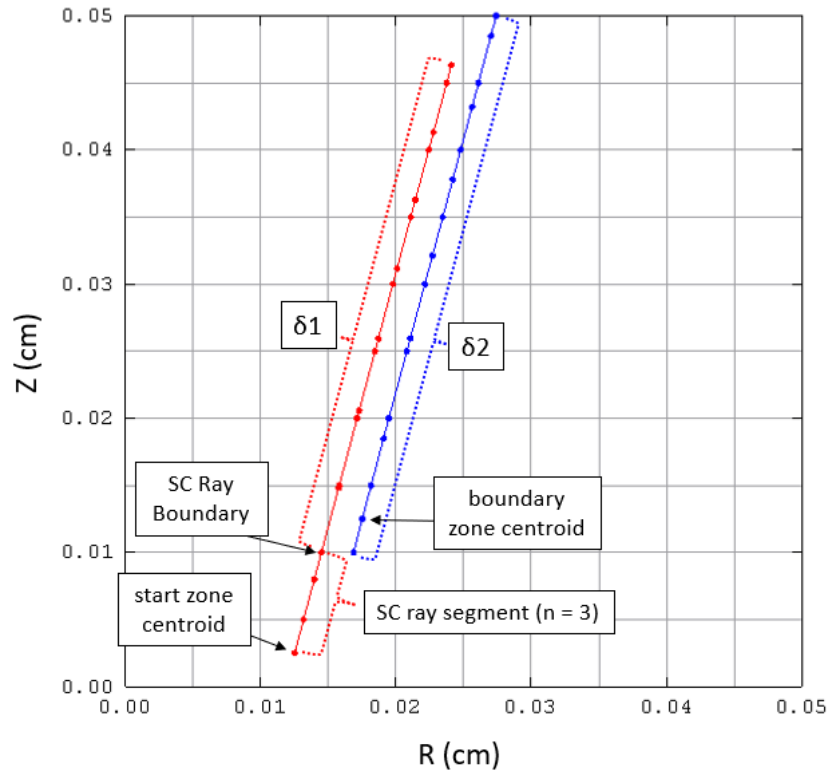


Figure 9. Lengths used for boundary value scaling factors for hotspot grid model in SC. Gridlines are plasma cell boundaries.

### Criteria for Omission of “Remainder” Ray Boundary Values

Remainder rays, i.e. rays which point toward solid angle other than the hotspot (and directly away from the hotspot), can sometimes take paths which end up close to, or even inside, the hotspot radius. This is partly because they tend to have few choices for boundary rays given the amount of subtended solid angle. In some cases, this can cause large amounts of extra intensity to be accumulated, causing large variation features in the  $K\alpha$  emission. To prevent this from happening, remainder rays track whether they come within a 20% tolerance of the hotspot radius. If a remainder ray enters this region, all “downstream” rays (i.e., rays who use that one for its boundary value, etc.) have their boundary value set to zero.

## **Choosing Hotspot Size**

Care should be taken in choosing the hotspot radius, since the subtended solid angle determines the weight given to the intensity calculated. If possible, the radius should be defined by a best guess as to where the radiation comes from (e.g., not just by a material boundary). E.g., emissivity could be studied vs. temperature and density conditions using PrismSPECT, and this could inform a hotspot radius choice based on the hydro conditions.

## **Reference**

1. Lathrop, K. D., Carlson, B. G.: "Discrete Ordinates Angular Quadrature of the Neutron Transport Equation," Los Alamos Scientific Laboratory, LA-3186 (1965).